BioMetals (2006) 19:143–157
DOI 10.1007/s10534-006-0003-2

Feo – Transport of ferrous iron into bacteria

Michaël L. Cartron[1], Sarah Maddocks[1], Paul Gillingham[2], C. Jeremy Craven[2] & Simon C. Andrews[1,*]
[1]*School of Biological Sciences (AMS Building), University of Reading, Whiteknights, Reading, RG6 6AJ, UK;* [2]*Department of Molecular Biology and Biotechnology, University of Sheffield, Firth Court, Western Bank, Sheffield, S10 2TN, UK; *Author for correspondence (E-mail: s.c.andrews@reading.ac.uk; Tel.: +44-118-378-8463; Fax: +44-118-931-0180)*

Received 18 December 2005; accepted 16 January 2006

Key words: G-protein, SH3, DtxR, MntR, Gate motif, transport, manganese, FeoA, FeoB, FeoC, Meo

Summary

Bacteria commonly utilise a unique type of transporter, called Feo, to specifically acquire the ferrous (Fe^{2+}) form of iron from their environment. Enterobacterial Feo systems are composed of three proteins: FeoA, a small, soluble SH3-domain protein probably located in the cytosol; FeoB, a large protein with a cytosolic N-terminal G-protein domain and a C-terminal integral inner-membrane domain containing two 'Gate' motifs which likely functions as the Fe^{2+} permease; and FeoC, a small protein apparently functioning as an [Fe–S]-dependent transcriptional repressor. We provide a review of the current literature combined with a bioinformatic assessment of bacterial Feo systems showing how they exhibit common features, as well as differences in organisation and composition which probably reflect variations in mechanisms employed and function.

Iron transport pathways in bacteria

The ability to acquire sufficient quantities of iron from the environment is vital for the majority of prokaryotes. This is particularly true for pathogens that must compete with the host iron-withdrawal response for their iron supplies. The transport systems that enable bacterial-iron acquisition have been the focus of much research since they contribute greatly to bacterial virulence and to gut colonisation proficiency of commensals (Andrews *et al.* 2003). Often, multiple iron transport pathways are present within a given bacterial species providing a range of specificities and affinities for various forms of environmental iron. The most common iron-transport pathways utilised by bacteria would appear to be those that enable uptake of ferric complexes (e.g. ferri-siderophores, haem and haem–protein complexes, ferric–transferrin/lactoferrin complexes, and ferric–citrate). For Gram-negative bacteria, such transporters generally consist of a TonB-ExbBD-dependent outer-membrane receptor, a periplasmic binding-protein, and an inner-membrane ABC permease complex. In addition, other types of iron transporter that import the free ferrous metal, are also employed by bacteria. These include the metal-ABC permeases and Nramp-like transporters, such as SitABCD and MntH (respectively) in *Salmonella* (Kehres *et al.* 2002; Zaharik *et al.* 2004). Such transporters tend to display specificity for divalent metals, particularly Fe^{2+} and Mn^{2+}, but may be primarily involved in the uptake of manganese, rather than iron. The major route for bacterial-ferrous-iron uptake would appear to be, in many cases, via Feo (*Ferr*ous iron transport). The Feo system appears to be unlike any other bacterial transporter. Given its importance and

novelty, surprisingly little research has been performed on Feo. However, recent studies have provided further insights into some of its structural and functional properties. Here, we review the current literature, recent structural advances and provide a bioinformatics analysis of the Feo systems of bacteria.

Discovery of Feo

Ferrous iron can be considered to be the preferred form of iron utilised by bacteria since, unlike the ferric form, it is relatively soluble (0.1 M for Fe^{2+} cf 10^{-18} M for Fe^{3+} at pH 7) allowing direct transport of the free metal. However, ferrous iron is only likely to predominate over ferric iron under reducing (anaerobic) conditions, or at low pH, conditions that favour ferrous iron stability. So unsurprisingly, ferrous iron transport is generally associated with bacteria growing under anaerobic–microaerophilic conditions, and possibly low pH. In addition, some bacteria are capable of actively reducing extracellular ferric iron in order to solublise it for the purpose of uptake, although little is known about the mechanism or components of extracellular-ferric iron reduction in bacteria (Cowart 2002). The first bacterial ferrous iron transport (Feo) system discovered was that of *Escherichia coli* K-12 (Hantke 1987), a facultative-anaerobic gut commensal. The K_m for Fe^{2+} uptake was ~0.5 μM (similar to the values, 0.54 and 0.31 μM, later measured for Feo system of the microaerophile, *Helicobacter pylori* and for *Porphyromonas gingivalis*, respectively; Velayudhan *et al.* 2000; Dashper *et al.* 2005) and the rate was found to increase by up to threefold following a shift from aerobic to anaerobic conditions. Thus, somewhat surprisingly, Fe^{2+} transport in *E. coli* occurs both aerobically and anaerobically, but is anaerobically induced. In addition, the rate of Fe^{2+} uptake was ~fourfold enhanced by inactivation of the *fur* gene which encodes the global iron-dependent transcriptional repressor, Fur. This indicated that *feo* expression is Fe^{2+}-Fur repressed (Hantke 1987). Feo activity was not affected by mutations in ferric iron uptake genes (*exbB*, *fhuF* or *tonB*), showing that Fe^{2+} uptake proceeds via a pathway distinct from that of Fe^{3+}.

E. coli mutants (*feo*) defective in import of ferrous iron were isolated using the antibiotic streptonigrin which generates toxic free radicals in the presence of iron and oxygen. Streptonigrin resistant (Sg^R) mutants often have lower intracellular iron levels caused by iron-transport defects (Hantke 1987). Sg^R mutants were generated under conditions where Fe^{2+} was the main iron source, using a *fur aroB* mutant in which Feo activity is high and siderophore biosynthesis absent. Desired mutants were selected by comparing growth of survivors in the presence and absence of citrate (*E. coli* can utilise ferric-dicitrate as an iron source). Isolates with reduced growth without citrate were found to exhibit impaired Feo activity (~tenfold lower Fe^{2+} transport rates). The *feo*$^-$ locus was subsequently cotransduced with a randomly introduced Tn*10* marker, from an original *feo*$^-$ isolate, into fresh backgrounds. The *feo*$^-$ locus was found to cause derepression of the Fe-Fur regulated *fhuF–lacZ* and *fiu–lacZ* fusions, presumably due to decreased cellular-iron accumulation caused by lack of Feo activity.

The *feo* locus was finally cloned and sequenced six years later (Kammler *et al.* 1993). Isolation of *feo*$^-$ complementing clones was not possible due to their instability. Cloning was therefore achieved by isolation of *feo*::Tn*5* mutants using an *fhuF–lacZ* fusion strain as a reporter of low intracellular Fe levels resulting from *feo* disruption. *Feo* mutants were distinguished from *tonB* or *fur* mutants (which would also cause increased *fhuF–lacZ* activity) on the basis of location in the *E. coli* genetic map (Kammler *et al.* 1993). The *feo*::Tn*5* region was then cloned and sequenced, and the chromosomal position determined (74.9 min, equivalent to 76.3 min within the current physical map of the *E. coli* chromosome; EcoGene data base).

Genetic organisation and control of the *feo* operon of *E. coli*

The nucleotide sequence of the *feo* locus of *E. coli* initially suggested the presence of two genes (*feoA* and *feoB*; Kammler *et al.* 1993) although it is now know to constitute three closely associated, co-polar (clockwise orientation) genes likely to form an operon, *feoABC* (Figure 1; Hantke 2003). The operon thus encodes three predicted proteins: FeoA, a small 75-residue hydrophilic protein; FeoB, a large 773-residue protein with an integral

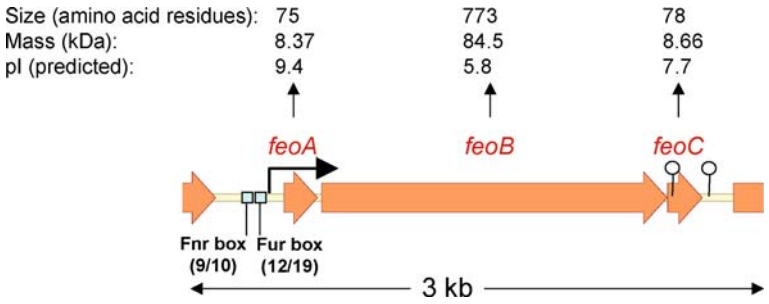

Figure 1. Organisation of the *feoABC* operon of *E. coli*. The predicted size, mass and pI of each of the *feo* translation products are indicated. The positions of putative transcriptional terminators are shown downstream of *feo B* and *feo C*. The stop codon of *feoA* and start codon of *feoB* are separated by just 16 bp; the stop and start codons of *feoB* and *feoC*, respectively, overlap. Predicted Fnr- and Fur-binding sites (matches to consensus sequences are shown), and a potential promoter (TTGctg-17-TATcAT) are indicated. Note that colour versions of *all* figures are available on line.

membrane domain (~270–773) likely to act as the ferrous permease; and FeoC (or YhgG), a small 78-residue hydrophilic protein found so far only associated with γ-proteobacterial Feo systems. Interestingly, no difference in Feo^- phenotype was observed for *feoA*::Tn*5* and *feoB*::Tn*5* mutants, indicating that either both genes are required for Feo activity, or that disruption of the upstream *feoA* interferes with expression of the downstream *feoB*. However, $^{55}Fe^{2+}$ uptake experiments showed a clear distinction between the *feoA* and *feoB* mutants: the *feoB* mutation virtually eliminated Fe^{2+} transport activity; whereas the *feoA*::Tn*5* insertion only reduced uptake by about 25% in a *fur* background (Kammler *et al*. 1993) possibly due to polar effects. In addition, expression of *feoB* from a plasmid resulted in enhanced rates of Fe^{2+} uptake both aerobically and anaerobically, confirming that Feo activity is not greatly O_2 inhibited. Experiments with a *feoA*-expressing plasmid were not reported. These results suggest that FeoB has the major role in Fe^{2+} uptake (Figure 2). The role of FeoA was unclear due to potential polar effects of the *feoA*::Tn*5* mutation on *feoB*, but at most it would appear to have a relatively minor enhancing effect on FeoB transport activity and have little if any transport function in the absence of FeoB (Figure 2).

Potential Fur and Fnr boxes were identified upstream of the *feoABC* operon which probably confer the observed Fe–Fur and O_2 dependence of Feo activity. The Fur box is appropriately located between predicted −35 and −10 boxes, whereas the Fnr box is at −91.5 bp with respect to the predicted promoter (Figure 1) suggesting Fnr would function as a class I activator for *feo* (Ebright 1993). A Fur-titration assay indicated that the *feo* promoter region does indeed possess a functional Fur box. Subsequently, experiments with a chromosomal *feoAB–lacZ* operon fusion showed an *fnr* mutation causes a fivefold reduction of *feo* expression under anaerobic, high-iron conditions suggesting that *feoABC* is anaerobically induced by Fnr, consistent with the presence of the Fnr box and the induction of Feo activity anaerobically. The *fnr* mutant demonstrated a six-fold induction in response to iron chelation indicating that Fnr does not contribute significantly to iron-dependent regulation of *feo* expression.

In vivo role of Feo

The above work clearly suggests that Feo would have an import role in iron uptake under the anaerobic-microaerophilic conditions of the gastro-intestinal tract. This possibility has now been confirmed in several bacteria. Both *E. coli* and *Salmonella feoB* mutants are attenuated in their ability to colonise the mouse intestine presumably due to their inability to transport ferrous iron within the anaerobic environment of the mouse intestine (Stojiljkovic *et al*. 1993; Tsolis *et al*. 1996). However, there have been contrasting reports on the role of Feo in systemic infection by *Salmonella*. In one case, a *feoB* mutation did not affect systemic infection (Tsolis *et al*.1996), whereas other work showed that *feoB* is required for full virulence in Nramp-deficient mice, although does not affect survival in macrophages (Boyer *et al*. 2002). The differences in these results may reflect differences in the *Salmonella* or mice

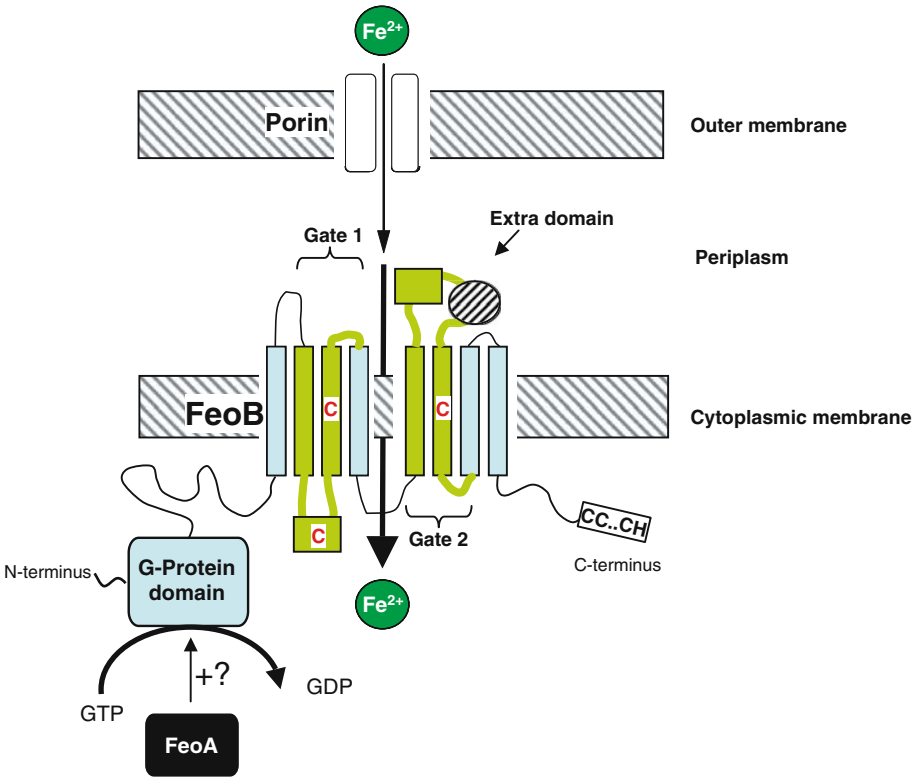

Figure 2. Schematic representation of ferrous iron uptake by Feo of *E. coli*. Extracellular Fe^{2+} is presumed to diffuse into the periplasm via undefined porins. It is then transported across the cytoplasmic membrane into the cytoplasm by FeoB through an apparent ATP/GTP-driven active transport process. The FeoB protein possesses a G-protein domain at its N-terminus and two 'Gate' motif regions (light green) within the membrane-embedded section. Highly conserved Cys residues are shown in red and a Cys/His-rich region at the C-terminus of FeoB (also found in several other FeoBs) is indicated. The 'extra' domain (insert found in *E. coli* FeoB and close relatives) is shown. The topology shown is based on that depicted in Figure 3 and is a prediction only. FeoA is thought to be required for maximal FeoB activity and is shown (speculatively) activating the GTPase function of FeoB.

strains employed (Boyer *et al.* 2002). Combining mutations in the Sit (an Mn^{2+} and Fe^{2+} transporter) and Feo systems resulted in complete avirulence, suggesting that these two systems both contribute to Fe^{2+} uptake *in vivo*. In the microaerophile, *H. pylori*, FeoB appears to provide the main route of iron uptake. It is required for *H. pylori* colonisation of mouse gastric mucosa, as well as for normal growth and iron-uptake under iron-restricted conditions (Velayudhan *et al.* 2000). In *Shigella flexneri*, a *feoB* mutation (or other single mutations in iron acquisition genes) had little impact on growth within Henle cells (Runyen-Janecky *et al.* 2003). However, when combined with mutations in other iron transporters (Sit or Iut – Mn^{2+}/Fe^{2+} and Fe^{3+}-aerobactin transporters, respectively) there was a clear growth defect indicating that multiple uptake systems (including Feo) contribute to *in vivo* iron acquisition for *S. flexneri*. FeoB is also required for intracellular growth of *Legionella pneumophila* (Robey & Cianciotto 2002) and for virulence of *P. gingivalis* (Dashper *et al.* 2005). Thus, various studies clearly establish an *in vivo* role for Feo in colonisation of the gut and in virulence.

The Feo proteins

FeoA

Co-conservation of FeoA and FeoB

Some 46% of the ~250 completely sequenced bacterial genomes (NCBI database, Sept 2005) possess genes specifying a Feo system (recognised by the presence of a gene encoding a protein with significant sequence similarity to the hydrophobic C-terminal region of FeoB) (see Figure 3 for a

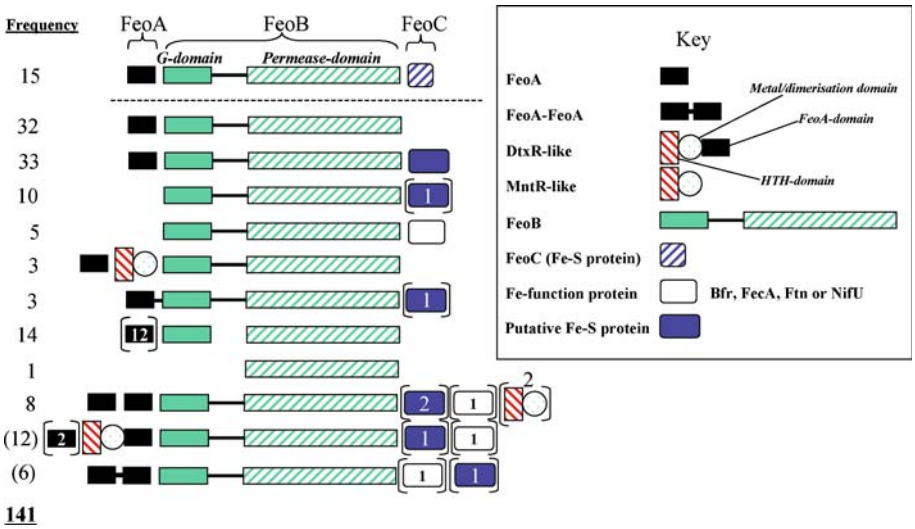

Figure 3. Comparison of the organisation of *feo* -gene regions in prokaryotes. The *feo* loci of the completely sequenced bacterial genomes (NCBI, Sept 05) were compared and grouped according to organisational similarity. The number of *feo* loci matching each of the organisational patterns is given ('frequency') as is the total number of *feo* loci discovered (141 from ~250 genomes). Frequency numbers in parentheses indicates that the order of genes differs, in some cases, from that displayed. Each rectangular or circular symbol represents a type of domain (see 'key' for details) and those in square parentheses only occur in some cases (the precise frequency is indicated by the associated number).

schematic representation of the genetic organisation of Feo-encoding systems). In most cases (80%), the *feoB* gene is associated with a *feoA* gene indicating that FeoA and FeoB have a close, interdependent functional relationship. There are 122 *feoA*-like genes in the NCBI database and all are adjacent to *feoB* genes indicating that FeoA functionality is strictly associated with FeoB interaction.

Homology with the SH3 domain of DtxR

The FeoA protein is relatively small being typically 75–85 amino acids in length (e.g. 75 residues and 8.4 kDa for FeoA of *E. coli*) (Figure 1). It has a hydrophilic amino acid sequence and there is no signal sequence apparent at its N-terminus, so it is likely to be located in the cytosol. FeoA proteins have an unusually high pI (e.g. 9.43 predicted for FeoA of *E. coli*) suggesting a potential to interact with the negatively charged macromolecules such as the cytoplasmic membrane (and it could therefore be a peripheral-membrane protein) or other proteins with negative charge.

Although the function and structure of FeoA are unknown, it bears weak amino-acid-sequence similarity to the C-terminal domain of DtxR and related proteins such as IdeR (Figure 4; Andrews *et al*. 2003; Pfam; Interpro). DtxR (the *d*iptheria *tox*in *r*egulator protein) functions as the major iron-responsive regulator in *Corynebacterium diphtheriae*. DtxR homologues (e.g. IdeR and SirR) are found in other high-GC-content Gram-positive bacteria (e.g. *Mycobacterium* and *Streptomyces*) where they have similar functions in serving as Fe-dependent repressors (Boyd *et al*. 1990; Tao *et al*. 1994; Oguiza *et al*. 1995; Dussurget *et al*. 1996; Hill *et al*. 1996). DtxR displays little or no sequence similarity to Fur, but like Fur, has an N-terminal helix-turn-helix DNA-binding domain (Pohl *et al*. 1998; 1999) followed by a central dimerisation domain containing two metal-binding sites one of which provides iron-sensing capability (Figure 5). Unlike Fur, it contains a third domain at the C-terminal end which is tethered to the rest of the protein by a flexible linker (Figure 5). This C-terminal domain is of unknown function but it has the same fold as the Src-Homology 3 (SH3) domain (originally identified as the non-catalytic N-terminal domain of Src tyrosine kinase; Cicchetti *et al*. 1992; D'Aquino & Ringe 2003). As mentioned above, it is this SH3-like domain that exhibits homology to FeoA. DtxR proteins are homologous with MntR proteins, Mn^{2+}-dependent repressors, found in *E. coli* and other bacteria

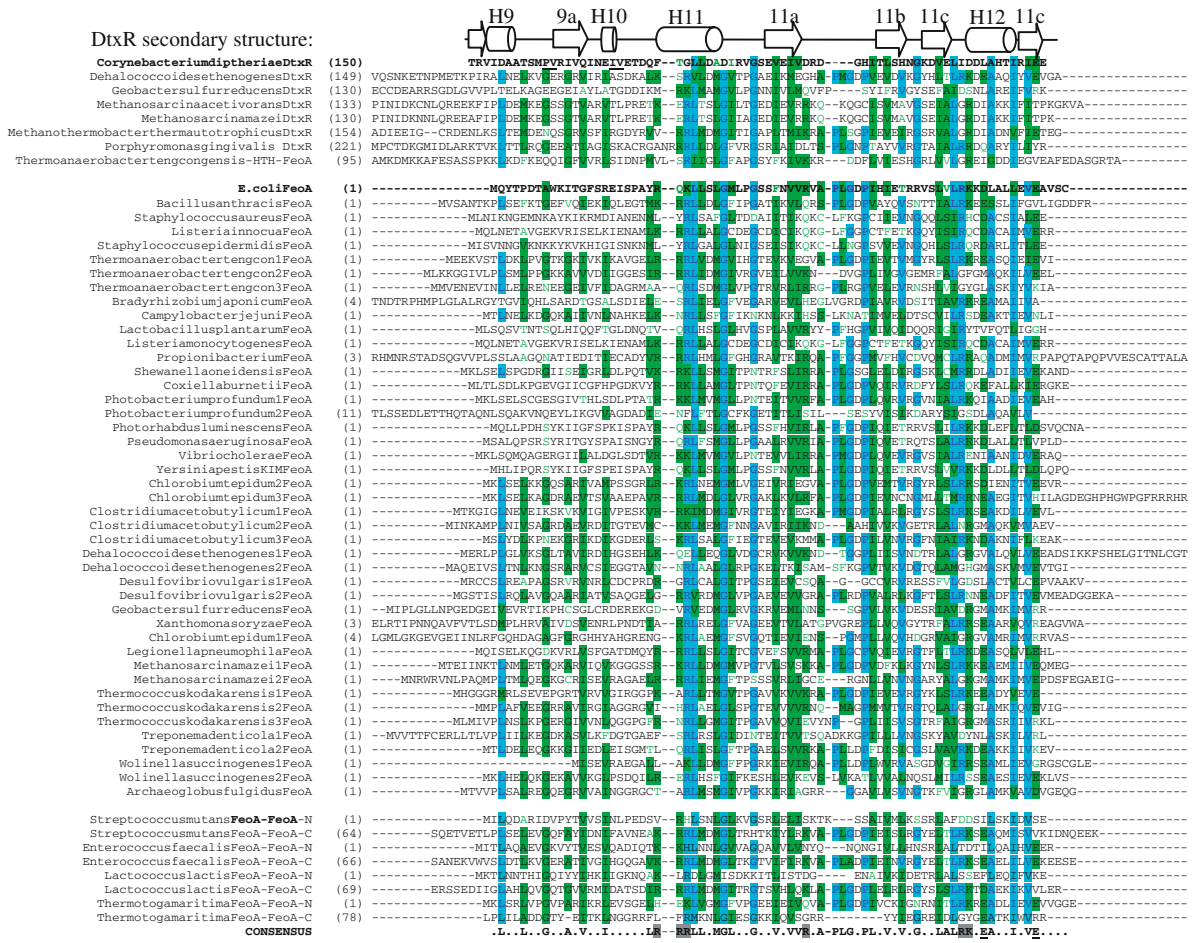

Figure 4. Multiple amino-acid-sequence alignment of FeoA and DtxR. The alignment includes: the C-terminal region of various DtxR proteins (top); various FeoA proteins (middle); and the N- and C-terminal halves of several FeoA–FeoA proteins (bottom). Note that many prokaryotes contain more than one FeoA and some corresponding examples are included in the alignment. Alignment was achieved with VectorNTI using default parameters, with some optimisation achieved by reference to Pfam. The degree of conservation is indicated (blue background, high; green background, moderate; green lettering, weak). The residue number is shown at the beginning of each sequence. The secondary structure of *C. diphtheriae* DtxR is shown above the alignment (cylinders,α-helices; arrows, β-strands) and regions where DtxR residues have been omitted to achieve optimal alignment are underscored. A consensus sequence is shown with positively and negatively charged residues highlighted and underscored, respectively.

(Patzer & Hantke 2001). Significantly, MntR, like Fur, lacks the C-terminal SH3/FeoA-like domain.

SH3 domains are found in a number of eukaryotic signalling (e.g. Ras-GTPase activating protein or GAP) and cytoskeletal proteins (e.g. myosin 1B). The domain functions in mediating protein-protein interactions required for processes such as subcellular localisation, cellular differentiation and cell proliferation. SH3 domains are composed of 50–70 residues that form a barrel with five anti-parallel β-strands (Musacchio *et al.* 1992a,b; 1994a,b; Mayer 2001). A characteristic cluster of conserved aromatic residues provides a hydrophobic site for interaction with target proteins, often at a 10-residue Pro-rich motif. FeoA and the SH3-domain of DtxR proteins have no clear sequence similarity with eukaryotic SH3-domain proteins, but their common fold does suggest a common role in mediating protein–protein interactions. This raises the possibility that FeoA interacts with its partner protein, FeoB, perhaps to mediate FeoB-dependent Fe^{2+}-uptake activity.

The multiple amino-acid alignment for the FeoA-DtxR family shows that residues between helices 11 and 12 are well conserved, with few insertions or deletions within the secondary structure elements (Figure 4). This supports the

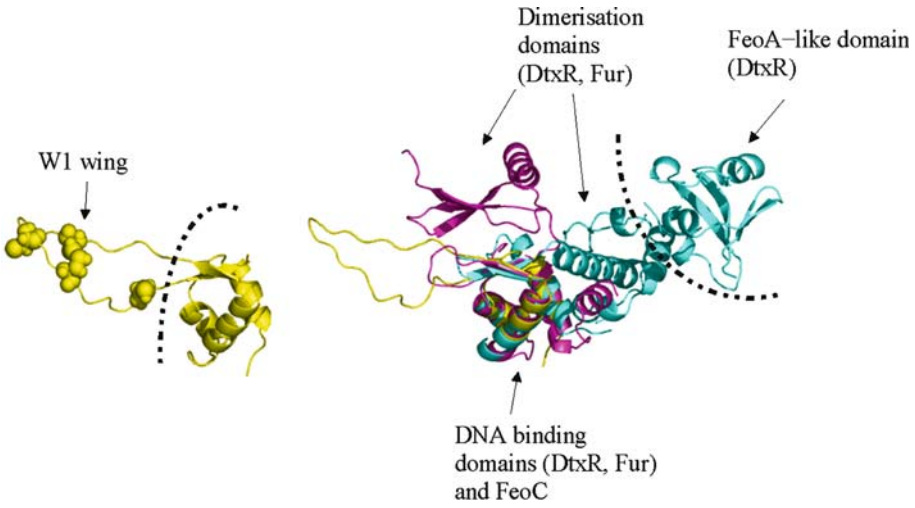

Figure 5. Cartoon representations of the structures of FeoC (left) and DtxR (right). Left: the FeoC structure was determined by NMR (PDB code 1nx7), and the W1 wing region was found to be disordered. A representative conformation is shown here. The four conserved Cys residues are indicated by space-filling. Right: the structured part of FeoC (yellow) is overlaid onto the DNA-binding domains of DtxR (cyan) and Fur (magenta) showing their similarity. In contrast, the structures and orientations of the dimerisation domains of DtxR and Fur are clearly distinct. The Feo-like SH3 domain of DtxR is marked. The structural similarity between the SH3 domain of DtxR and FeoA is further supported by the threading analysis with the FeoA sequence (www.sbg.bio.ic.ac.uk/~3dpssm).

notion that FeoA and the SH3-domain of DtxR are structurally analogous. One major area of insertion/deletion is seen within this otherwise well conserved region, within a loop between β-strands 11b and 11c which would, once again, be consistent with the suggested structural topology. In contrast, the N-terminal region (helices 9 to 10) is quite poorly conserved suggesting this region may be less important for FeoA function. Those residues that are conserved within FeoA-family members are mainly hydrophobic or have small side chains (Gly and Ala) suggesting that they have structural roles (Figure 4). However, there are six relatively well conserved positively charged residues, three of which form a cluster in helix 11. These would contribute significantly to the high predicted pI of the FeoA proteins and may have a role in protein–protein interaction. Surprisingly, there are only two (partially) conserved negatively, charged residues (Figure 4). These are potential Fe^{2+} ligands (note, there is no evidence that FeoA binds metal) and are located towards the C-terminal end of the protein (Figure 4). There are no conserved His or Cys residues (also potential Fe^{2+} ligands) within the FeoA family.

Alternative FeoA organisations

Interestingly, there are at least eight examples in the databases where there are two FeoA proteins associated with a single FeoB-encoding gene (Figure 3). In such cases, the two FeoA proteins are not closely related which suggests that they may have evolved to provide somewhat different functions. In addition, there are six cases where a single polypeptide consists of two FeoA domains fused together (Figure 3). The N- and C-terminal halves of these FeoA–FeoA proteins display little sequence similarity, and indeed, the N-terminal halves generally show only weak sequence similarity to other FeoA proteins. It is unclear what purpose the additional FeoA domain might provide but, as for the cases where two separate FeoA proteins are found together, their distinctiveness is suggestive of functional specialisation. In three other cases, the *feoA*- and *feoB*-open-reading frames are fused in-frame generating a predicted FeoA–FeoB hybrid translation product (Figure 3). This fusion is consistent with a role for FeoA involving interaction with FeoB. A FeoA–FeoB fusion of this sort is found in the Feo1 system of *P. gingivalis* (two Feo systems are present in this organism, Feo1 and Feo2) which has been shown to be involved in Fe^{2+} uptake (Dashper *et al.* 2005). Note that the presence of multiple Feo systems is relatively common: there are 25 cases of two Feo systems; and two cases of three Feo systems (Figure 8).

Interestingly, there are also ten Feo systems where the only FeoA domain is provided by an associated DtxR-like protein (also described as a MntR-FeoA fusion protein; Dashper *et al*. 2005). Recent work has shown that the DtxR-associated Feo2 system of *P. gingivalis* is a specific Mn^{2+} transporter, rather than an Fe^{2+} transporter (Dashper *et al*. 2005). This suggests that the other DtxR-associated Feo systems are also likely to be Mn^{2+} importers (here designated 'Meo'), rather than true Feo (ferrous iron) transporters. It also indicates that the Meo/Feo-associated DtxR proteins have dual functions as Mn^{2+}-dependent repressors and as components of the 'Meo' transport pathway. Thus, under high cytosolic Mn^{2+} concentrations Meo-associated DtxR could bind at the *meo* promoter repressing expression of the Meo system, but under low Mn^{2+} levels it could be free to associate with the MeoB protein to potentially activate Mn^{2+} uptake. This proposed dual functionality may well extend to the DtxR proteins of the high-GC Gram positives, although these bacteria generally do not possess any Feo-like system and so any protein-protein interaction mediated by the C-terminal DtxR domain within these bacteria must involve some other partner protein, such as an alternative iron-transporter. The absence of any possible interaction between these DtxR proteins and FeoB may well explain the weak sequence similarity between their C-terminal domains and FeoA (BLAST searches generally fail to detect any similarity). However, in the cases where the DtxR and FeoB proteins are associated, the sequence similarity between the C-terminal DtxR domain and FeoA is relatively high (e.g. for the DtxR of *Dehalococcoides ethenogenes* again FeoA of *E. coli*, BLAST e score $= 8 \times 10^{-13}$).

FeoB

Overall structure

FeoB is the major component of the Feo system. It is likely to act as the permease through which ferrous iron is transported into the cell. For *E. coli*, the FeoB protein is composed of a hydrophilic N-terminal domain (FeoB-N; residues 1 to 270) and a C-terminal integral-membrane domain (FeoB-C; residues ~271–773,) predicted to consist of eight transmembrane α-helices (Figure 6). This organisation seems to be preserved across species, although there are examples were the N-terminal and C-terminal domains are separately encoded (Figure 3) and one example where the FeoB-N region is completely absent, and also the number of predicted transmembrane helices may vary between species (Marlovitis *et al*. 2002).

The hydrophilic N-terminal 'G-protein' region

An important insight into the mechanism of action of FeoB was revealed by the finding that the N-terminal hydrophilic domain contains a G-protein region (residues 1 to ~160) followed by a poorly conserved region of uncertain function (160 to ~270) (Marlovitis *et al*. 2002). This observation suggests that the N-terminal 'G-protein region' has GTPase activity, as observed for the homologous small regulatory G-proteins of eukaryotes. G-proteins are characterised by five consecutive GTPase motifs (G1-G5) (Sprang 1997; Marlovitis *et al*. 2002) but although motifs G1-G4 are clearly identifiable for FeoB, the poorly conserved G5 motif could not be defined (Marlovitis *et al*. 2002). Subsequently, experiments with the isolated N-terminal domain of *E. coli* FeoB (FeoB-N, residues 1 to 274) confirmed the anticipated GTP-binding ability (using a non-hydrolysable fluorescent analogue of GTP, mant-GMPPNP) and showed lack of affinity for an ATP analogue, demonstrating a high degree of nucleotide specificity. FeoB-N was able to hydrolyse GTP to GDP but, as for the eukaryotic regulatory G-proteins, hydrolysis was extremely slow (50% hydrolysis was achieved after ~6 h at 37 °C) with a k_{cat} of ~0.0015 s^{-1} at 37 °C. No hydrolysis was observed with ATP, consistent with the binding studies. Full-length FeoB exhibited similar GTPase activity to FeoB-N indicating that the activity of the G-protein domain is not enhanced by the C-terminal domain under the conditions tested. Kinetic measurements gave off- and on-rate constants of 1.4 s^{-1} and 0.36 μM^{-1} s^{-1}, respectively, for mant-GMPPNP binding to FeoB-N, and a K_d of ~4 μM. This affinity is three-orders of magnitude weaker than observed for the eukaryotic small-regulatory G-proteins (e.g. p21-ras and the α-subunit of heterotrimeric G proteins) but closely matches that of prokaryotic GTPases such as Era, CgtA of *Caulobacter crescentus* and FtsY in *E. coli* (Brown 2005). The binding and release kinetics of FeoB-N for GDP were found to be so

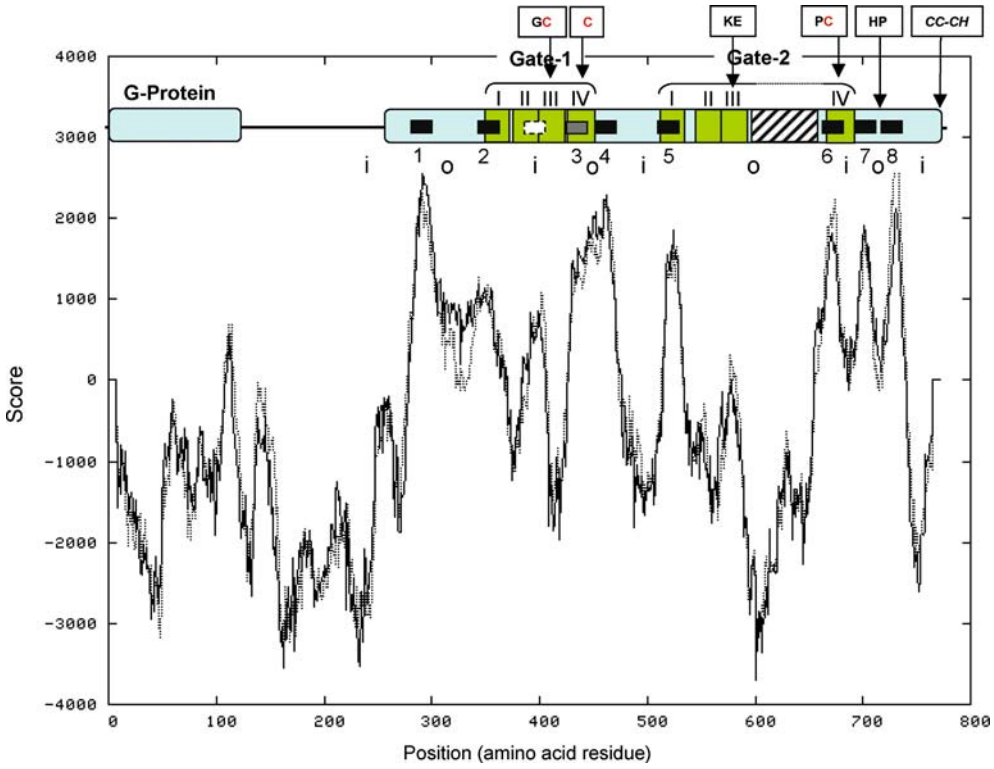

Figure 6. Predicted transmembrane helices and structural organisation of the *E. coli* FeoB. The transmembrane-helix prediction (black/grey bars, 1–8) was generated using the TMpred program at EMBnet. The hydropathy plot was generated using the Kyte & Doolittle options of ProtScale at ExPASy. The white broken bar indicates a TMpred-predicted spanner in the Gate-1 region that is not included in the topology prediction as it is not predicted in the Gate-2 region nor in NupC. The grey bar indicates a Gate-1 spanner not predicted by TMpred but included here since it is predicted for NupC and Gate-2. Orientation (i, inside; and o, outside the cytoplasm) is indicated. Locations of the Gate-1 and Gate-2 (divided into four blocks, I–IV) motifs are shown in green. An extra region of ~70 residues, found in *E. coli* FeoB and closely related FeoB proteins, but not in more distantly related FeoB, is indicated as a hatched region. Highly conserved Cys residues are shown in red, and several other conserved residues are also shown, including a Cys/His-rich motif (CC-CH) at the C-terminus of the *E. coli* protein and a few other FeoBs.

fast that the rates could not be measured by stopped-flow approaches. This was a surprise as the small regulatory G-proteins characteristically exhibit slow release of GDP.

The role of the G4 motif (residues 120–123, NxxD) in GTP binding was confirmed by site-directed mutagenesis showing that the D123N alteration resulted in lack of GTP-analogue binding and conversion to specificity for a xanthosine analogue. The lack of involvement of a potential alternative G4 motif (residues 91–94) was also demonstrated using a D94N FeoB-N variant. The importance of the G-protein domain in Fe^{2+} uptake by FeoB was indicated by using an Fe-regulated *fhuF–lacZ* reporter to provide an indication of *E. coli* iron status. In this way, a *feoB* deletion strain carrying the *fhuF–lacZ* reporter was complemented with plasmids expressing either a 'wildtype' or a D123N mutant FeoB. Neither the D123N-FeoB construct nor the vector control allowed repression of the *fhuF–lacZ* fusion by external iron whereas, in contrast, the wildtype-FeoB construct enabled repression at ≥100 μM iron. Even when iron levels were raised to 400 μM, the D123N-FeoB construct still failed to allow iron to enter the cell sufficiently to cause repression of the fusion indicating that FeoB transport activity is strongly dependent on its G-protein domain.

There are a large number of eukaryotic G-proteins known of which Ras is the archetype. G-proteins have important cellular functions in proliferation, differentiation, malignancy and cytoskeletal architecture. The Ras-like G-proteins act as regulators controlling cellular processes in

response to their GTP/GDP status: the GTP-bound forms are active whereas the GDP-bound forms are inactive. The activity of these proteins is tightly controlled by two other types of protein, GEFs and GAPs. The 'guanine-nucleotide exchange factors' (GEFs) activate Ras-like proteins by mediating nucleotide release and GTP loading in response to appropriate signals. 'GTPase-activating proteins' (GAPs) deactivate Ras-like proteins by accelerating the hydrolysis of the bound GTP. In comparison to the eukaryotic G-proteins, FeoB-N thus has some unusual properties. It possesses low affinity for GTP coupled with a low hydrolysis rate, but it has a fast release rate for GDP. G-proteins involved in signalling normally have high rates of GTP hydrolysis combined with strong GDP binding in order to produce a stable GDP-bound form in the 'off' state. The properties of FeoB-N suggest that, if it indeed is regulatory in function, it might be predominantly in the GTP-bound 'on' state *in vivo*. FeoB-N might be expected to require some factor or event to trigger its conversion to the GDP-bound 'off' state, as mentioned above for eukaryotic G-proteins. It may be significant that GAPs, like FeoA, possess an SH3-like domain (Schwartz 2005; Siderovski & Willard 2005). GAP's interact with GTP-binding proteins in an SH3-dependent manner and stimulate GTPase activity. They essentially switch GTPases on and off by regulating the change between the active GTP-bound and inactive GDP-bound form. This raises the intriguing possibility that FeoA acts as GAP in triggering high GTPase activity for FeoB-N (as speculatively represented in Figure 2). However, it is also possible that this effect is mediated in some other way, such as by the C-terminal hydrophobic region of FeoB, or through interaction with a small ligand such as Fe^{2+}. Indeed, any mechanism governing the rate of Feo-transport activity in response to intracellular ferrous iron concentration would be an attractive possibility since this would help to ensure that the cell does not suffer from sudden and rapid influxes of excess iron under conditions where environmental iron levels fluctuate widely. However, currently, there is no evidence for any control of Feo-transport activity at the biochemical level, only at the transcriptional level.

An alternative possibility is that FeoB-N has a role in energising FeoB-mediated Fe^{2+} uptake through GTP hydrolysis. Such a role would clearly require much higher hydrolysis rates than so far exhibited (Marlovitis *et al*. 2002; Hantke 2003) and would thus imply the potential to activate FeoB-N in some fashion (e.g. as described above). However, there is experimental evidence suggesting that Feo activity in *H. pylori* is ATP dependent (Velayudhan *et al*. 2000) which contradicts the above hypothesis. Thus, currently, the purpose of the G-protein domain, the role of FeoA and the mode of energisation for Feo-mediated Fe^{2+} uptake are all unclear.

The hydrophobic C-terminal region and Gate motifs

The hydrophobic C-terminal region of FeoB contains two homologous 'Gate' motifs (Gate 1 and Gate 2; Figure 7) originally identified in transmembrane-nucleoside transporters (e.g. human CNT1 and *E. coli* NupC; note the nucleoside transporters contain just one recognised Gate motif in contrast to the two present in FeoB) (Loewen *et al*. 1999; Pfam). Prediction of the topology of FeoB suggests that the two Gate motifs have opposite orientations within the membrane. This organisation would be reminiscent of the iron permease of yeast, Ftr1p, which also possesses a duplicated motif (the metal-binding 'RExLE' motif; Severance *et al*. 2004) with opposite orientations within the membrane. There are a number of conserved residues within the FeoB transmembrane domain, the most interesting of which are two Cys residues, each located identically in segment 4 of Gates 1 and 2 (Figure 6 and 7). This feature seems unique to the Gate motifs of FeoB, since the equivalent residue in the nucleoside transporters is non-conserved (Pfam). Cys residues are good ligands for soft Lewis acids (such as Fe^{2+}) suggesting that these two conserved Cys residues could be involved in metal binding during the transport process Many nucleoside transporters are Na^{+} dependent which raises the possibility that the Gate motif functions in metal translocation for both the nucleoside transporters (with specificity for hard Lewis bases) and FeoB.

The Gate 2 region possesses a large insertion of around 70 residues located between segments III and IV (Figures 6 and 7). This insertion is only present in a subset of FeoB proteins mainly from γ-proteobacteria. The proteins within this FeoB subset also contain a C-terminal extension of $\sim$40 residues with a predicted transmembrane helix followed by a *potential* Fe^{2+}-binding Cys–His rich region presumed to be located in the cytosol (Figures 6 and 7). This feature is some-

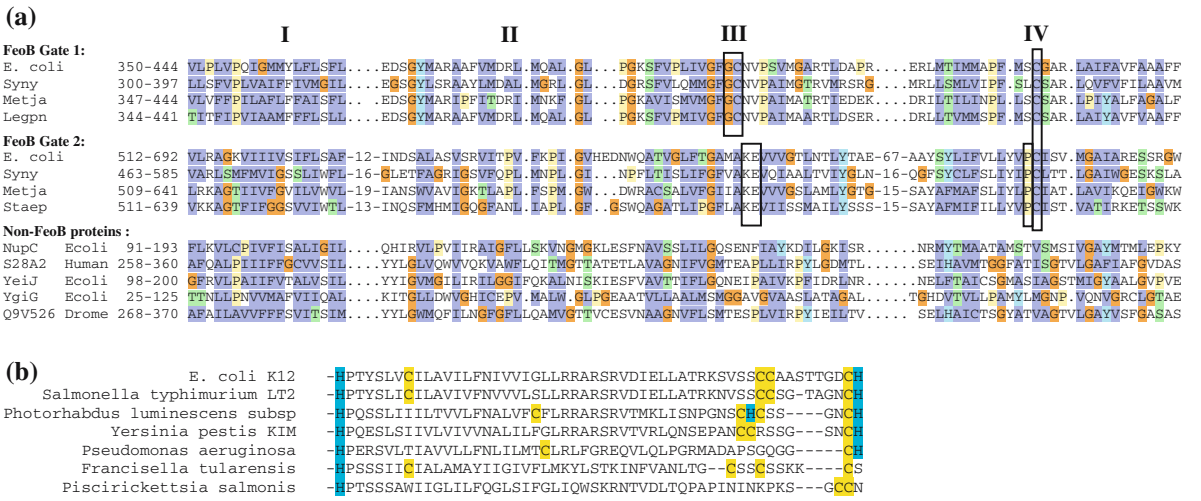

Figure 7. Multiple amino-acid sequence alignments of FeoB fragments. (a) The Gate regions of FeoB and other non-FeoB proteins (sequence coordinates are shown). Conserved residues are from the original Pfam alignment and are coloured using the ClustalX scheme (orange, G; yellow, P; blue, A, V, L, I, M, F, W; green, S, T, N, Q; red, D, E, R, K; cyan, H, Y). Conserved residues of interest are boxed and the number of residues deleted in order to achieve optimal alignment is indicated in each case. The Gate motif is divided into 4 conserved blocks (I–IV). Syny, *Synechocystis* sp.PCC 6803; Metja, *Methanococcus jannaschii*; Legpn, *Legionella pneumophila*; Staep, *Staphylococcus epidermidis*; Drome, *Drosphophilla melanogaster*. The 'non-FeoB proteins' are all from the nucleoside-transporter group, other than YgiG which is a smaller protein of unclear function containing just a Gate motif. (b) The C-terminal region of γ-proteobacterial FeoB proteins showing the Cys/His-rich region.

what similar to the metal-binding motifs (CxxC), possibly having a chaperone function, found in the metal-transporting P-type ATPases (Rensing *et al.* 1999). This Cys–His rich region in FeoB may have a similar role, or could be more directly involved in metal-dependent FeoB-activity control or Fe^{2+} translocation.

FeoB phylogeny and multiple Feo's

A phylogenetic tree generated using a subset of FeoB sequences highlights the presence of multiple FeoB proteins within some bacteria. In such cases, the corresponding FeoB proteins are normally located in quite different parts of the tree, indicating that they have diverged evolutionarily and thus may serve different functions (Figures 8 and S1). The region highlighted and boxed (Figures 8 and S1) consists of a major branch of the FeoB family that includes the MeoB (FeoB2) protein of *P. gingivalis*. Significantly, most of the bacteria that contain two or more FeoB-like proteins have one FeoB in the boxed branch and one in the remaining part of the tree (e.g. *P. gingivalis*, *Bacillus* spp., *Staphylococcus* spp., *Pelobacter propionicus*, *Methanosarcinia* spp., *Clostridium tetani* and *Geobacter sulfurreducens*; Figures 8 and S1). In addition, the part of the tree outside the box contains the functionally defined Fe^{2+} transporters (labelled in Figures 8 and S1); none are found in the boxed region. This suggests that the boxed branch may consist of a major FeoB subfamily specialised for Mn^{2+} transport. If so, this would provide an explanation for the presence of multiple Feo-like systems within some bacteria.

FeoC – a novel Fe–S dependent transcriptional regulator of feoABC?

Interestingly, in *E. coli* the *feoB* gene precedes a gene called *yhgG* (or *feoC*) which is also found similarly located within the *feo* locus of other γ-proteobacteria (Figures 1 and 3). The stop codon of *feoB* overlaps the start codon of *feoC* suggesting that the two genes are co-operonic and translationally coupled. Our (McHugh, Hinton and Andrews, unpublished) microarray data show that *feoC* is Fe-Fur repressed (as for *feoAB*). Thus, it would appear that the *feo* operon consists of three co-regulated genes, *feoABC*. The predicted 78-residue amino acid sequence of the FeoC protein indicates that it is hydrophilic with a pI of 7.7 (Figure 1). Multiple-alignment of the FeoC proteins (15 examples in the NCBI database, Sept 2005) shows that they possess four conserved Cys

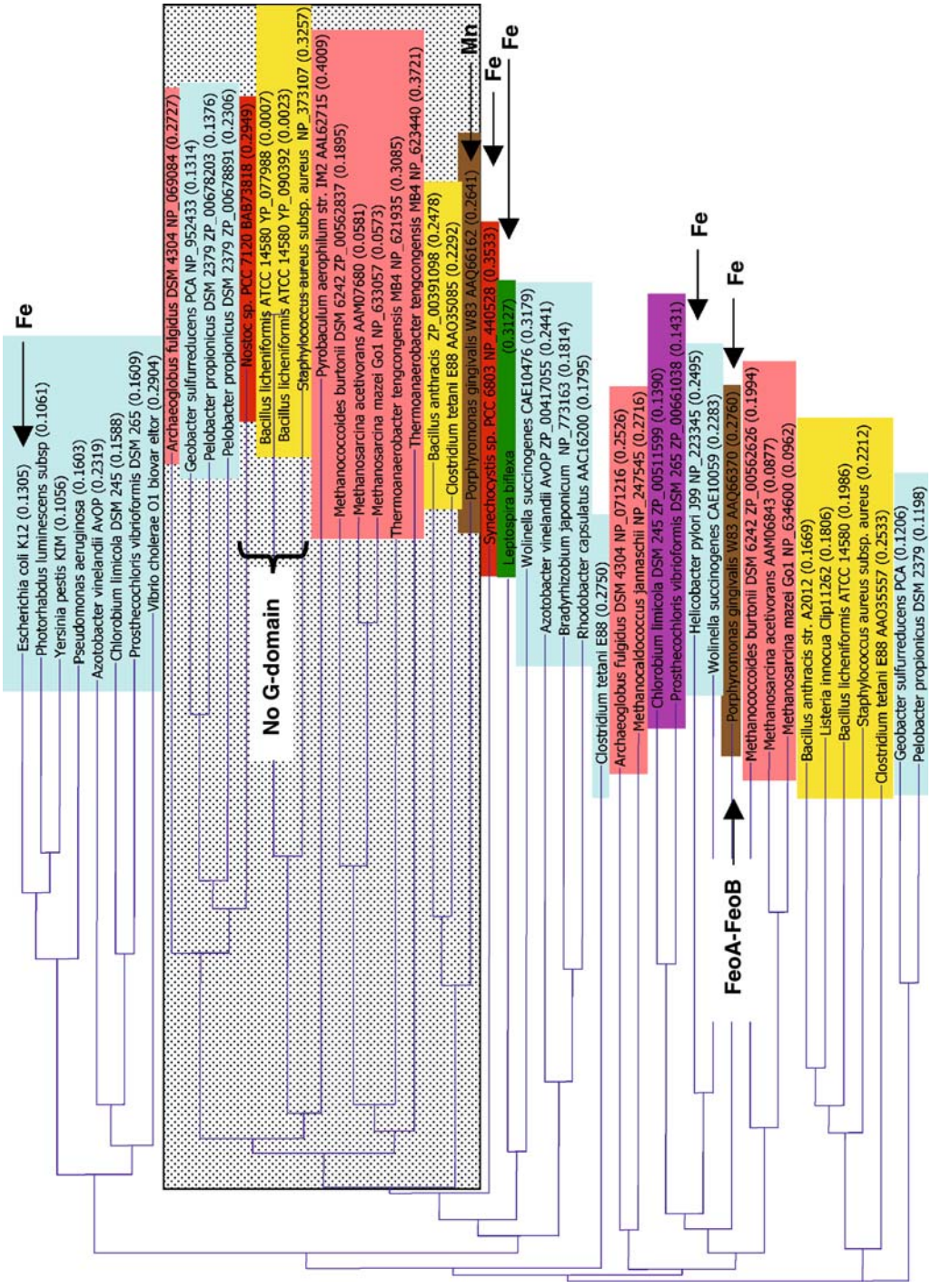

Figure 8. Phylogenetic tree of FeoB. A multiple-amino-acid-sequence alignment of a representative subset of FeoB sequences (49, or 132 for Figure S1) was used to generate a phylogenetic tree using the VectorNTI program (standard options). Branch lengths are proportional to distance (values are given at the end of each branch). Coloured boxes indicate bacterial phylogeny: acidobacteria, dark blue; actinobacteria, grey; aquificae and thermotoga, no colour; bacteroidetes, brown; chlorobi, purple; chloroflexi, light green; cyanobacteria, red; deinococcus-thermus, dark purple; euryarchaeota and crenarchaeota, pink; firmicutes, yellow; proteobacteria, light blue; and spirochaetes, dark green. The boxed region indicates a major branch of the FeoB family possibly specialised for Mn^{2+} transport. Defined 'Fe' and 'Mn'-transporting systems are indicated (e.g. for *Leptospira biflexa* and *Synechocystis*; Louvel *et al.* 2005; Hirokazu *et al.* 2001) and those proteins lacking the G-protein domain or consisting of FeoA–FeoB fusions are labelled. See 'Supplementary Information' for a more complete version of this tree (Figure S1).

residues (**C**xxG**x**C**K**x**CP**x$_{4\text{-}7}$**C**) likely to provide a binding site for an [Fe–S]-cluster (Figure 9). Furthermore, the solution structure of FeoC has recently been deposited in the Protein Data Bank by the Northeastern Structural Genomics Consortium (Figure 5; PDB code 1xn7) revealing that the protein is a monomer with a winged-helix fold (Gajiwala *et al*. 2000) within its N-terminal region. This fold belongs to the family of helix-turn-helix folds and is normally DNA (sometimes RNA) binding in function (http://scop.mrc-1mb.cam.ac.uk/scop/data/scop.b.b.g.e.html). Indeed, the protein is predicted (MotifScan) to possess a LysR-like winged-helix motif at its N-terminus (Figure 9) supporting a likely role as a transcriptional repressor. Similar motifs are present in the DNA-binding domains of Fur and DtxR (Figure 5). Compared to other known winged-helix structures, FeoC has a much larger W1 "wing" loop. This C-terminal wing loop is poorly structured and quite flexible. It contains the four Cys residues to which an Fe–S cluster is proposed to bind (no metal is present in the solved FeoC structure). It is probable that the binding of an Fe–S cluster at the C-terminal Cys-residues would result in structural reorganisation of this region triggering a change in DNA-binding affinity. FeoC therefore has properties suggesting that it would function as a transcriptional regulator, directly controlling *feoABC* expression. Several other transcriptional regulators also possess Fe–S clusters as redox (SoxR, Fnr) or Fe sensors (IscR and RirA) raising the possibility of similar ability for FeoC (Green & Paget 2004; Todd *et al*. 2002). Note that although FeoC shares the same general fold as the DNA-binding N-terminal domains of

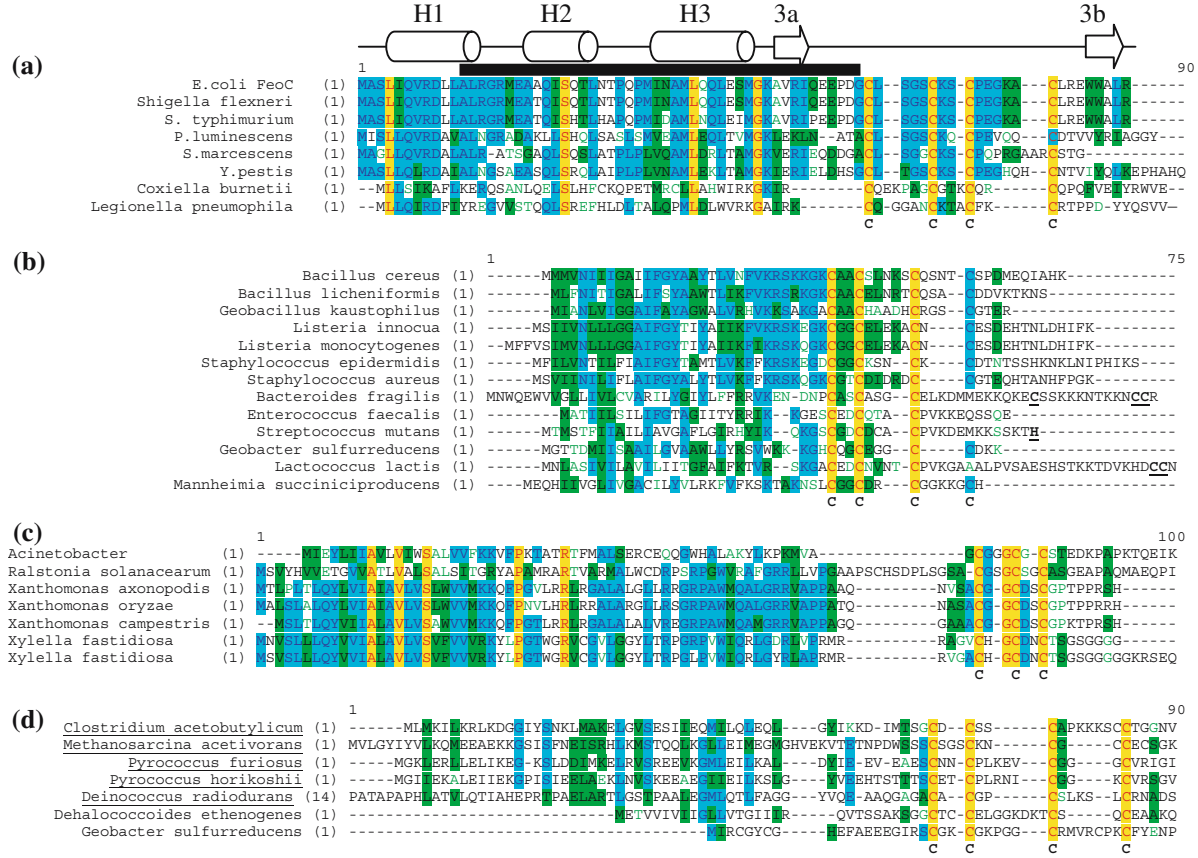

Figure 9. Multiple amino-acid-sequence alignment of FeoC (a) and other small Cys-rich proteins encoded within *feo* clusters (b, c and d). The defined secondary-structural elements of FeoC are shown (as for Figure 4) and the predicted LysR-like DNA-binding region (MotifScan) is indicated by a black bar. Proteins predicted to be helix-turn-helix DNA-binding proteins are indicated by underscoring of the corresponding species name (ind). Conserved Cys residues potentially acting as Fe–S cluster ligands are indicated below each alignment. Highly, moderately and weakly conserved residues are indicated by yellow, blue and green shading, respectively. Note that alignment is based upon overall amino-acid sequence similarity and/or similarity in Cys residue spacings.

Fur and DtxR, it does not display any significant sequence similarity to these proteins.

Although genes encoding FeoC-like proteins are only found in the γ-proteobacteria, many other *feo*-gene clusters encode small, unknown proteins that, like FeoC, also possess Cys-rich clusters within their C-terminal regions which have the potential to bind an Fe–S cluster (or metal) (Figures 3 and 9). These proteins may also function as metal/redox-dependent transcriptional regulators, as proposed for FeoC. Indeed, several (see underscoring in Figure 9D) are predicted to be DNA-binding proteins (Swiss-Prot database).

Conclusion

The Feo system is a unique divalent metal transporter found in a wide range of prokaryotic species. It is generally composed of three major units: an SH3-like domain; a G-protein domain; and an integral-membrane domain containing two Gate motifs. These are found in various polypeptide/subunit organisations. The transport mechanism employed, and the specific roles of the three major Feo units, are currently unknown. There is good bioinformatics evidence suggesting that, often, a dedicated (metal-specific) transcriptional regulator is associated with the corresponding operon which is likely to regulate expression in response to metal availability. Two types of Feo system are now known, one that is Fe^{2+} specific and another (Meo) that is Mn^{2+} specific. It is possible that the Feo family is divided into two evolutionary distinct branches, consisting of Mn and Fe specific transporters. This may provide an explanation for the frequent occurrence of two (or more) evolutionarily distinct Feo-like systems within a single bacterium.

Acknowledgements

We thank the BBSRC for provision of a project grant to SCA and both BBSRC and Nanomagnetics for supporting a CASE studentship to SM.

References

Andrews SC, Robinson AK, Rodriguez-Quinones F. 2003 Bacterial iron homeostasis. *FEMS Microbiol Rev* **27**, 215–37.

Boyd J, Oza MN, Murphy JR. 1990 Molecular cloning and DNA sequence analysis of a diphtheria *tox* iron-dependent regulatory element (*dtxR*) from *Corynebacterium diphtheriae*. *Proc Natl Acad Sci USA* **87**, 5968–72.

Boyer E, Bergevin I, Malo D, Gros P, Cellier MF. 2002 Acquisition of Mn(II) in addition to Fe(II) is required for full virulence of *Salmonella enterica* serovar Typhimurium. *Infect Immun* **70**, 6032–42.

Brown ED. 2005 Conserved P-loop GTPases of unknown function in bacteria: an emerging and vital ensemble in bacterial physiology. *Biochem Cell Biol* **83**, 738–746.

Cicchetti P, Mayer BJ, Thiel G, Baltimore D. 1992 Identification of a protein that binds to the SH3 region of Abl and is similar to Bcr and GAP-rho. *Science* **257**, 803–806.

Cowart RE. 2002 Reduction of iron by extracellular iron reductases: implications for microbial iron acquisition. *Arch Biochem Biophys* **15**, 273–81.

D'Aquino J, Ringe D. 2003 Determinants of the Src homology domain 3-like fold. *J Bacteriol* **185**, 4081–4086.

Dashper SG, Butler CA, Lissel JP, Paolini RA, Hoffmann B, Veith PD, O'Brien-Simpson NM, Snelgrove SL, Tsiros JT, Reynolds EC. 2005 A novel *Porphyromonas gingivalis* FeoB plays a role in manganese accumulation. *J Biol Chem* **280**, 28095–102.

Dussurget O, Rodriguez M, Smith I. 1996 An *ideR* mutant of *Mycobacterium smegmatis* has derepressed siderophore production and an altered oxidative-stress response. *Mol Microbiol* **22**, 535–44.

Ebright RH. 1993 Transcription activation at class I CAP-dependent promoters. *Mol Microbiol* **8**, 797–802.

Gajiwala KS, Burley SK. 2000 Winged helix proteins. *Curr Opin Struct Biol* **10**, 110–116.

Green J, Paget MS. 2004 Bacterial redox sensors. *Nat Rev Microbiol* **2**, 954–66.

Hantke K. 1987 Ferrous iron transport mutants in *Escherichia coli* K-12. *FEMS Microbiol Lett* **44**, 53–57.

Hantke K. 2003 Is the bacterial ferrous iron transporter FeoB a living fossil. *Trends Microbiol* **11**, 192–195.

Hill PJ, Cockayne A, Landers P, Morrissey JA, Sims CM, Williams P. 1998 SirR, a novel iron-dependent repressor in *Staphylococcus epidermidis*. *Infect Immun* **66**, 4123–4129.

Hirokazu K, Hagino N, Grossman AR, Ogawa T. 2001 Genes essential to iron transport in the cycanobacterium *Synechocystis* sp Strain PCC 6803. *J Bacteriol* **183**, 2779–2784.

Kammler M, Schon C, Hantke K. 1993 Characterisation of the ferrous iron uptake system of *Escherichia coli*. *J Bacteriol* **175**, 6212–6219.

Kehres DG, Janakiraman A, Hauch JM, Maguire ME. 2002 SitABCD is the alkaline Mn^{2+} transporter of *Salmonella enterica* serovar Typhimurium. *J Bacteriol*. **184**, 3159–3166.

Loewen SK, Ng AM, Yao SY, Cass CE, Baldwin SA, Young JD. 1999 Identification of amino acid residues responsible for the pyrimidine and purine nucleoside specificities of human concentrative Na^{+} nucleoside cotransporters hCNT1 and hCNT2. *J Biol Chem* **274**, 24475–24484.

Louvel H, Saint Girons I, Picardeau M. 2005 Isolation and characterisation of FecA- and FeoB-mediated iron acquisition systems of the spirochete *Leptospira biflexa* by random insertional mutagenesis. *J Bacterial* **187**, 3249–3254.

Marlovits TC, Haase W, Herrmann C, Aller SG, Unger VM. 2002 The membrane protein FeoB contains an intramolecular G protein essential for Fe(II) uptake in bacteria. *Proc Natl Acad Sci* **99**, 16243–16248.

Mayer BJ. 2001 SH3 domains: complexity in moderation. *J Cell Science* **114**, 1253–1263.

Musacchio A, Gibson T, Lehto VP, Saraste M. 1992a SH3 – an abundant protein domain in search of a function. *FEBS Lett* **307**, 55–61.

Musacchio A, Noble M, Pauptit R, Wierenga R, Saraste M. 1992b Crystal structure of a Src-homology 3 (SH3) domain. *Nature* **359**, 851–854.

Musacchio A, Saraste M, Wilmanns M. 1994a High-resolution crystal structures of tyrosine kinase SH3 domains complexed with proline-rich peptides. *Nat Struct Biol* **1**, 546–551.

Musacchio A, Wilmanns M, Saraste M. 1994b Structure and function of the SH3 domain. *Prog Biophys Mol Biol* **61**, 283–297.

Oguiza JA, Tao X, Marcos AT, Martin JF, Murphy JR. 1995 Molecular cloning, DNA sequence analysis, and characterization of the *Corynebacterium diphtheriae* DtxR homolog from *Brevibacterium lactofermentum*. *J Bacteriol* **Vol**, 465–467.

Patzer SI, Hankte K. 2001 Dual repression by Fe^{2+}-Fur and Mn^{2+}-MntR of the *mntH* gene, encoding an NRAMP-like Mn^{2+} transporter in *Escherichia coli*. *J Bacteriol* **183**, 4806–13.

Pohl E, Holmes RK, Hol WG. 1998 Motion of the DNA-binding domain with respect to the core of the diphtheria toxin repressor (DtxR) revealed in the crystal structures of apo- and holo-DtxR. *J Biol Chem* **273**, 22420–7.

Pohl E, Holmes RK, Hol WG. 1999 Crystal structure of the iron-dependent regulator (IdeR) from *Mycobacterium tuberculosis* shows both metal binding sites fully occupied. *J Mol Biol* **285**, 1145–56.

Rensing C, Ghosh M, Rosen BP. 1999 Families of Soft-Metal-Ion-Transporting ATPases. *J Bacteriol* **181**, 5891–5897.

Robey M, Cianciotto NP. 2002 *Legionella pneumophila feoAB* promotes ferrous iron uptake and intracellular infection. *Infect Immun* **70**, 5659–5669.

Runyen-Janecky LJ, Reeves SA, Gonzales EG, Payne SM. 2003 Contribution of the *Shigella flexneri* Sit, Iuc, and Feo iron acquisition systems to iron acquisition in vitro and in cultured cells. *Infect Immun* **71**, 1919–28.

Schwartz M. 2005 Rho signalling at a glance. *J Cell Science* **117**, 5447–5458.

Severance S, Chakraborty S, Kosman DJ. 2004 The Ftr1p iron permease in the yeast plasma membrane: orientation, topology and structure-function relationships. *Biochem J* **380**, 487–496.

Siderovski DP, Willard FS. 2005 The GAP's, GEF's and GDI's of heterotrimeric G-protein alpha subunits. *Int J Biol Sci* **1**, 51–66.

Sprang SR. 1997 G protein mechanisms: insights from structural analysis. *Annu Rev Biochem* **66**, 639–678.

Stojiljkovic I, Cobeljic M, Hantke K. 1993 *Escherichia coli* K-12 ferrous iron uptake mutants are impaired in their ability to colonize the mouse intestine. *FEMS Microbiol Lett* **108**, 111–5.

Tao X, Schiering N, Zeng HY, Ringe D, Murphy JR. 1994 Iron, DtxR, and the regulation of diphtheria toxin expression. *Mol Microbiol* **14**, 191–197.

Todd JD, Wexler M, Sawers G, Yeoman KH, Poole PS, Johnston AW. 2002 RirA, an iron-responsive regulator in the symbiotic bacterium *Rhizobium leguminosarum*. *Microbiology* **148**, 4059–4071.

Tsolis RM, Baumler AJ, Heffron F, Stojiljkovic I. 1996 Contribution of TonB- and Feo-mediated iron uptake to growth of *Salmonella typhimurium* in the mouse. *Infect Immun* **64**, 4549–4556.

Velayudhan J, Hughes NJ, McColm AA, Bagshaw J, Clayton CL, Andrews SC, Kelly DJ. 2000 Iron acquisition and virulence in *Helicobacter pylori*: a major role for FeoB, a high-affinity ferrous iron transporter. *Mol Microbiol* **37**, 274–286.

Zaharik ML, Cullen VL, Fung AM, Libby SL, Kujat Choy SL, Coburn B, Kehres DG, Maguire ME, Fang FC, Finlay BB. 2004 The Salmonella enterica Serovar Typhimurium divalent cation transport systems MntH and SitABCD are essential for virulence in an $Nramp1^{G169}$ murine typhoid model. *Infect Immun* **72**:5522–5525.